Tunable Radiationless Energy Transfer in $Eu[Au(CN)_2]_3 \cdot 3H_2O$ by High Pressure

Hartmut Yersin,* Dietrich Trümbach, and Johann Strasser

Institut für Physikalische und Theoretische Chemie, Universität Regensburg, D-93040 Regensburg, Germany

Howard H. Patterson*

Department of Chemistry, University of Maine, Orono, Maine 04469

Zerihun Assefa

Transuranium Research Group, Oak Ridge National Laboratory, Oak Ridge, Tennessee 37831-6375

Received November 30, 1997

The title compound consists of two-dimensional layers of $[Au(CN)_2]^-$ complexes alternating with layers of Eu^{3+} ions. Due to this structure type, the lowest electronic transitions of the dicyanoaurates(I) exhibit an extreme red shift of $\Delta\bar{\nu}_{max}/\Delta p = -130 \pm 10$ cm^{-1}/kbar under high-pressure application at least up to ≈60 kbar ($T = 20$ K), while the shifts of the different Eu^{3+} transitions lie between −0.70 and −0.94 cm^{-1}/kbar. At ambient pressure, the usually very intense emission of the dicyanoaurates(I) is completely quenched due to radiationless energy transfer to the Eu^{3+} acceptors. As a consequence, one observes a strong emission from Eu^{3+}, which is assigned to stem mainly from $^5D_0$ but also weakly from $^5D_1$. At $T = 20$ K, $^5D_3$ seems to be the dominant acceptor term. It is a highlight of this investigation that, with increasing pressure, the emission from the dicyanoaurate(I) donor states can continuously be tuned in by tuning off the resonance condition (spectral overlap) for radiationless energy transfer to $^5D_3$. With further increase of pressure, successively, $^5D_2$ and $^5D_1$ become acceptor terms, however, being less efficient. Interestingly, $^5D_0$ does not act as an acceptor term even with maximum spectral overlap. Between 30 and 60 kbar, when only the $^7F_0 \rightarrow {}^5D_1$ acceptor absorption overlaps with the donor emission, one finds a linear dependence of the (integrated) $^5D_0$ emission intensity on the spectral overlap integral, as is expected for resonance energy transfer. As the dominant transfer mechanism, the Dexter exchange mechanism is proposed. Besides the high-pressure studies of the Eu^{3+} line structure at $T = 20$ K, the Eu^{3+} emission is also investigated at $T = 1.2$ K ($p = 0$ kbar) by time-resolved emission spectroscopy, which strongly facilitates the assignments of the emitting terms.

1. Introduction

$M[Au(CN)_2]$ compounds (e.g., with $M^+ = K^+$, Cs^+, Tl^+) have been the subject of increasing interest due to their two-dimensional layered structures and their interesting emission properties.[1−9] These structures consist of layers of $[Au(CN)_2]^-$ complexes alternating with layers of M^+ ions, which are in several cases coordinated with water molecules.[10−13] The distances between the gold ions within the layers are relatively short and change with the cation M^+. For example, the Au^+ ions are separated by 3.64 Å (at $T = 300$ K) for the potassium compound,[10] while the shortest Au−Au separation is only 3.11 Å for M = Cs.[11] On the other hand, the separations between the layers are of the order of 8 Å.[11] This structure type indicates the occurrence of important two-dimensional electronic interactions between the $[Au(CN)_2]^-$ units. Indeed, the optical absorption spectrum of the $[Au(CN)_2]^-$ ion in aqueous solution shows absorption bands only at energies higher than 40 000 cm^{-1}, while the $M[Au(CN)_2]$ crystals have their absorption bands shifted to lower energies by as much as 20 000 cm^{-1} (e.g., see refs 1 and 4). These shifts are ascribed in a first approximation to the formation of electronic energy bands, and the resulting band gap is energetically strongly lowered compared to the HOMO−LUMO separation of the complexes.[1,4,9]

(1) Patterson, H. H.; Roper, G.; Biscoe, J.; Ludi, A.; Blom N. *J. Lumin.* **1984**, *31/32*, 555.
(2) Markert, J. T.; Blom, N.; Roper, G.; Perregaux, A. D.; Nagasundaram, N.; Corson, M. R.; Ludi, A.; Nagle, J. K.; Patterson, H. H. *Chem. Phys. Lett.* **1985**, *118*, 258.
(3) Nagle, J. K.; LaCasce, J. H., Jr.; Dolan, P. J., Jr.; Corson, M. R.; Assefa, Z.; Patterson, H. H. *Mol. Cryst. Liq. Cryst.* **1990**, *181*, 359.
(4) Assefa, Z.; DeStefano, F.; Garepapaghi, M. A.; LaCasce, J. H., Jr.; Ouellette, S.; Corson, M. R.; Nagle, J. K.; Patterson, H. H. *Inorg. Chem.* **1991**, *30*, 2868.
(5) Fischer, P.; Ludi, A.; Patterson, H. H.; Hewat, A. W. *Inorg. Chem.* **1994**, *33*, 62.
(6) Fischer, P.; Mesot, J.; Lucas, B.; Ludi, A.; Patterson, H. H.; Hewat, A. *Inorg. Chem.* **1997**, *36*, 2791.
(7) LaCasce, J. H., Jr.; Turner, W. A.; Corson, M. R.; Dolan, P. J., Jr.; Nagle, J. K. *Chem. Phys.* **1987**, *118*, 289.
(8) Patterson, H. H. In *Electronic and Vibronic Spectra of Transition Metal Complexes. II;* Yersin, H., Ed.; Topics in Current Chemistry; Springer-Verlag: Berlin, 1997; Vol. 191, 59.
(9) Yersin, H.; Riedl, U. *Inorg. Chem.* **1995**, *34*, 1642.
(10) Rosenzweig, A.; Cramer, D. T. *Acta Crystallogr.* **1959**, *12*, 709.
(11) Blom, N.; Ludi, A.; Bürgi, H.-B.; Tichy, K. *Acta Crystallogr.* **1984**, *C40*, 1767.
(12) Blom, N.; Ludi, A.; Bürgi, H.-B. *Acta Crystallogr.* **1984**, *C40*, 1770.
(13) Assefa, Z.; Shankle, G.; Patterson, H. H.; Reynolds, R. *Inorg. Chem.* **1994**, *33*, 2187.

S0020-1669(98)00252-3 CCC: $15.00
Published on Web 06/05/1998

In addition, exciton effects are also important and strongly determine the properties of the low-lying energy states.[9] Interestingly, application of high pressure allows one to red-shift these states by extremely large values, which lie in the order of 2×10^2 cm^{-1}/kbar.[9,14]

Usually, the M[Au(CN)$_2$] compounds exhibit a very intense and broad emission from the [Au(CN)$_2$]$^-$ layers. However, if the cation M$^+$ = $^1/_3$ Eu^{3+} is selected, the dicyanoaurate(I) emission is totally quenched, but one observes intense Eu^{3+} lines. This effect was studied recently at different temperatures by Patterson and co-workers[13,15] and was ascribed to the occurrence of an effective radiationless energy transfer from the [Au(CN)$_2$]$^-$ layers, representing the donors, to the Eu^{3+} acceptors. This results in an emission from the $^5D_1$ and $^5D_0$ states of Eu^{3+}. As the acceptor term at low temperature ($T <$ 40 K) the $^5D_3$ excited state of Eu^{3+} was proposed, whereby the energy transfer to this term quenches the donor emission.[13]

It is an interesting question, on which we want to focus in this investigation, whether the extreme pressure-induced red shift of the donor states (layer states) can be used to tune the radiationless energy transfer to a situation in which other Eu^{3+} acceptor terms become dominant and to see whether the [Au(CN)$_2$]$^-$ layer emission can even be brought to appear by tuning off the radiationless energy transfer. Similar experiments have, to our knowledge, only been carried out by Yersin and co-workers[16−18] for the Eu^{3+} and Sm^{3+} salts of the tetracyanoplatinates(II). Indeed, as will be shown below, these effects can be found in Eu[Au(CN)$_2$]$_3$·3H$_2$O. It is a further object of this investigation to analyze the time dependence of the Eu^{3+} emission and to study line shifts under high pressure.

2. Experimental Section

Eu[Au(CN)$_2$]$_3$·3H$_2$O was prepared by addition of a stoichiometric amount of Eu(NO$_3$)$_3$·6H$_2$O (Alfa) to an aqueous solution of KAu(CN)$_2$ (Pfaltz and Bauer). The Eu(NO$_3$)$_3$·6H$_2$O solution was slowly added to the aqueous solution of KAu(CN)$_2$. The container was covered with paraffin to reduce the rate of evaporation. Then, the mixture was left undisturbed for several days. Light yellow crystals of Eu[Au(CN)$_2$]$_3$·mH$_2$O were collected and washed with distilled water and dried.[13] The content of crystal water was remeasured. We obtained a larger value (m = 3) than reported in ref 13.

Emission spectra at different pressures were recorded using similar equipment to that described in refs 19−21. For excitation of the samples in the high-pressure cell, an argon ion CW laser was used (Coherent Innova 90). All spectra were corrected for the spectral response of the monochromator and the photomultiplier (EMI 9659 QB S-20 extended, cooled to −30 °C). The monochromator (Spex 1404) read-out was calibrated to ±1 cm^{-1} by a low-pressure argon lamp. As the high-pressure cell, we used a modified sapphire cell of Bridgman's opposed anvil type. An inconel gasket with a small centric hole (diameter 0.4 mm), which represents the pressure chamber, was placed between two sapphire pistons. The pressure medium was paraffin oil. The pressure within the cell was determined by the pressure-induced shift of the R_1 line of small ruby crystals, which were located near the sample in the pressure chamber. The whole high-pressure cell was placed into a liquid-He combicryostat.

The time-resolved measurements were performed at 1.2 K. This temperature was achieved by pumping off the He (Leybold-Heraeus BBK 100 cryostat). As the excitation source, a Nd:YAG laser (SL803 Spectron, pulse width ≈ 12 ns, repetition rate 20 Hz) pumped dye laser (Lambda Physik FL 2000, modified to a spectral resolution of 0.15 cm^{-1} by Radiant Dyes) was used. Emission decay curves were registered with a fast multiscaler combined with a multichannel data processor (multiscaler 7885 and multichannel data processor, FAST ComTec, D-82041 Oberhaching, Germany). The time-resolved spectra were recorded with a gated photon counter (Stanford Research Systems, model SR 400).

3. Results and Discussion

3.1. Characterization of the Electronic Structures of the Donor States. The low-energy states of the dicyanoaurates(I) may be traced to the Au 5d,6s HOMO and the Au 6p, CN π^* LUMO, respectively. Due to the electronic interaction within the two-dimensional layers, energy bands develop, giving in the one-electron approximation valence and conduction bands. The resulting band gap, however, is in most cases not equal to the emission energy, since usually the excited electron in the conduction band interacts with the hole created in the valence band. Thus, the two particles, electron and hole, form excitons, which are energetically stabilized with respect to the band gap energy. The corresponding excited states are not confined to a specific complex unit. They are delocalized over the layers. Thus, the resulting energy level diagram may be described by a ground state and an energetically relatively broad exciton band, having its lower band edge (lowest lying state) much lower than the band gap energy. For example, for the tetracyanoplatinates(II), which exhibit in many respects similar spectroscopic properties,[22−27] an exciton stabilization energy of ≈4000 cm^{-1} was found (for Ba[Pt(CN)$_4$]·4H$_2$O).[26] Such a situation is common for solid-state compounds (e.g. see refs 28 and 29). However, the lowest states of the M[Au(CN)$_2$] compounds exhibit properties of localized states unlike the model described above. This is evidenced by a relatively large zero-field splitting of the low-lying triplet sublevels of the order of 50 cm^{-1} and the long emission lifetime of the order of several 10^2 μs.[2,4,30,31] (For further details with respect to the localization see ref 9.) Again, this behavior is similar to the properties of the M$_2$[Pt(CN)$_4$]·nH$_2$O compounds, for which it has been shown that a localization is induced by a shrinkage of the metal−metal separation upon excitation by a so-called self-trapping process.[24,25,27] Presumably, such a process is also important for the localization of the low-lying states of the dicyanoaurates(I). For completeness, it is mentioned that a similar behavior with respect to the shrinkage of the metal−metal separation has been reported for the excited states of [Pt$_2$(P$_2$O$_5$H$_2$)$_4$]$^{4-}$.[32−34] However, unlike the case of the tetracyanoplatinates(II), there

(14) Strasser, J.; Yersin, H.; Patterson, H. H. Submitted for publication.
(15) Assefa, Z.; Patterson, H. H. *Inorg. Chem.* **1994**, *33*, 6194.
(16) Yersin, H.; von Ammon, W.; Stock, M.; Gliemann, G. *J. Lumin.* **1979**, *18/19*, 774.
(17) Yersin, H.; Stock, M. *J. Chem. Phys.* **1982**, *76*, 2136.
(18) Yersin, H.; Gliemann, G. *Ann. N.Y. Acad. Sci.* **1978**, *313*, 539.
(19) Yersin, H.; Gliemann, G. *Messtechnik (Braunschweig)* **1972**, *80*, 99.
(20) Stock, M.; Yersin, H. *Chem. Phys. Lett.* **1976**, *40*, 423.
(21) Yersin, H.; Huber, P.; Gietl, G.; Trümbach, D. *Chem. Phys. Lett.* **1992**, *199*, 1.
(22) Interrante, L. V.; Messmer, R. P. In *Extended Interactions between Metal Ions in Transition Metal Complexes*; Interrante, L. V., Ed.; ACS Symposium Series 5; American Chemical Society: Washington, DC, 1974; p 382.
(23) Interrante, L. V.; Messmer, R. P. *Chem. Phys. Lett.* **1974**, *26*, 225.
(24) Rössler, U.; Pertzsch, B.; Yersin, H. *J. Lumin.* **1981**, *24/25*, 437.
(25) Rössler, U.; Yersin, H. *Phys. Rev.* **1982**, *B26*, 3187.
(26) Eichhorn, M.; Willig, F.; Yersin, H. *Chem. Phys. Lett.* **1981**, *81*, 371.
(27) (a) Gliemann, G.; Yersin, H. *Struct. Bonding* (*Berlin*) **1985**, *62*, 87. (b) Yersin, H.; Habilitationsschrift, Universität Regensburg, 1979.
(28) Hellwege, K.-H. *Einführung in die Festkörperphysik*; Springer-Verlag: Berlin, 1976; p 495ff.
(29) Burns, G. *Solid State Physics;* Academic Press: Orlando, FL, 1985; p 498ff.
(30) LaCasce, J. H.; Turner, W. A.; Corson, M. R.; Dolan, P. J.; Nagle, J. K. *Chem. Phys.* **1987**, *118*, 289.
(31) Riedl, U. Ph.D. Thesis, Universität Regensburg, 1992.
(32) Rice, S. F.; Gray, H. B. *J. Am. Chem. Soc.* **1983**, *105*, 4571.
(33) Roundhill, D. M.; Gray, H. B.; Che, C.-M. *Acc. Chem. Res.* **1989**, *22*, 55.
(34) Thiel, D. J.; Livins, P.; Stern, E. A.; Lewis, A. *Nature* **1993**, *362*, 40.

are indications that the situation for the dicyanoaurates(I) is additionally complicated by a tendency toward the formation of $[Au(CN)_2]_n^{n-}$ clusters already in the ground state. These cluster regions seem to exhibit reduced metal−metal distances in comparison to the regular crystallographic distances. This behavior has been proposed in ref 9 and is supported also by the present investigation (see section 3.4).

In summary, the lowest excited states of the dicyanoaurate(I) layers, being the donor states, represent long-lived triplets. Their energies are strongly lowered compared to those of the single $[Au(CN)_2]^-$ complex due to two-dimensional solid-state interactions. But due to $[Au(CN)_2]_n^{n-}$ cluster formation and exciton self-trapping effects, these donor states seem to be spatially localized.

3.2. High-Pressure-Induced Red Shift of the Donor Emission. The emission energies of the dicyanoaurates(I) exhibit an extremely large red shift under application of high pressure.[9,14] Values up to $\Delta\bar{\nu}_{max}/\Delta p = -200$ cm^{-1}/kbar are found, for example, for the potassium salt.[9] This behavior displays again the similarity between the $M[Au(CN)_2]$ and the $M_2[Pt(CN)_4]\cdot nH_2O$ compounds, whereby the tetracyanoplatinates(II) exhibit even larger shifts. For example, for $Mg[Pt(CN)_4]\cdot 7H_2O$, a value of $\Delta\bar{\nu}_{max}/\Delta p = -320$ cm^{-1}/kbar has been observed, representing one of the largest values hitherto reported for crystalline compounds.[35,36] The occurrence of such large values is a consequence (i) of relatively high compressibilities of the in-plane[6] or in-chain[35,36] metal−metal separations and (ii) of the large increase of wave function overlap of the molecular orbitals, which are responsible for the formation of the electronic energy bands, with a reduction of the metal−metal separation.[22,25,37−42]

At first sight, the pressure-induced shift of the low-lying energy states of the dicyanoaurate(I) layers of $Eu[Au(CN)_2]_3\cdot 3H_2O$ is difficult to determine, since at ambient pressure the corresponding emission is totally quenched.[13] However, for p $\gtrsim$ 10 kbar and at $T = 20$ K, a very weak emission occurs and grows in with increasing pressure (Figure 1). This effect, representing the highlight of this investigation, is a consequence of a pressure-induced tuning off of the radiationless energy transfer from the dicyanoaurate(I) donors to the Eu^{3+} acceptors. This behavior will be discussed in detail in section 3.4. Here, it is only applied to determine the shift of the emission peak energy under application of high pressure. Figure 2 shows that the maximum of the donor emission is shifted from ≈22 500 cm^{-1} at $p = 13$ kbar to nearly 16 000 cm^{-1} at about 60 kbar. A linear plot gives a value of $\Delta\bar{\nu}_{max}/\Delta p = -130 \pm 10$ cm^{-1}/kbar. This value is similar to those found for $Cs[Au(CN)_2]$ and $Cs_2Na[Au(CN)_2]_3$ of −150 and −120 cm^{-1}/kbar, respectively.[9]

For all dicyanoaurates investigated,[9,14] the red shift of the emission energies with pressure application is at least up to about 15 kbar well approximated by a linear plot. Thus, it is reasonable to extrapolate the straight line of Figure 2 to zero pressure, giving a value of 23 600 ± 300 cm^{-1}. At this energy, one would expect to find the maximum of the emission band of the "donor" (at $T = 20$ K), if no energy transfer occurred.

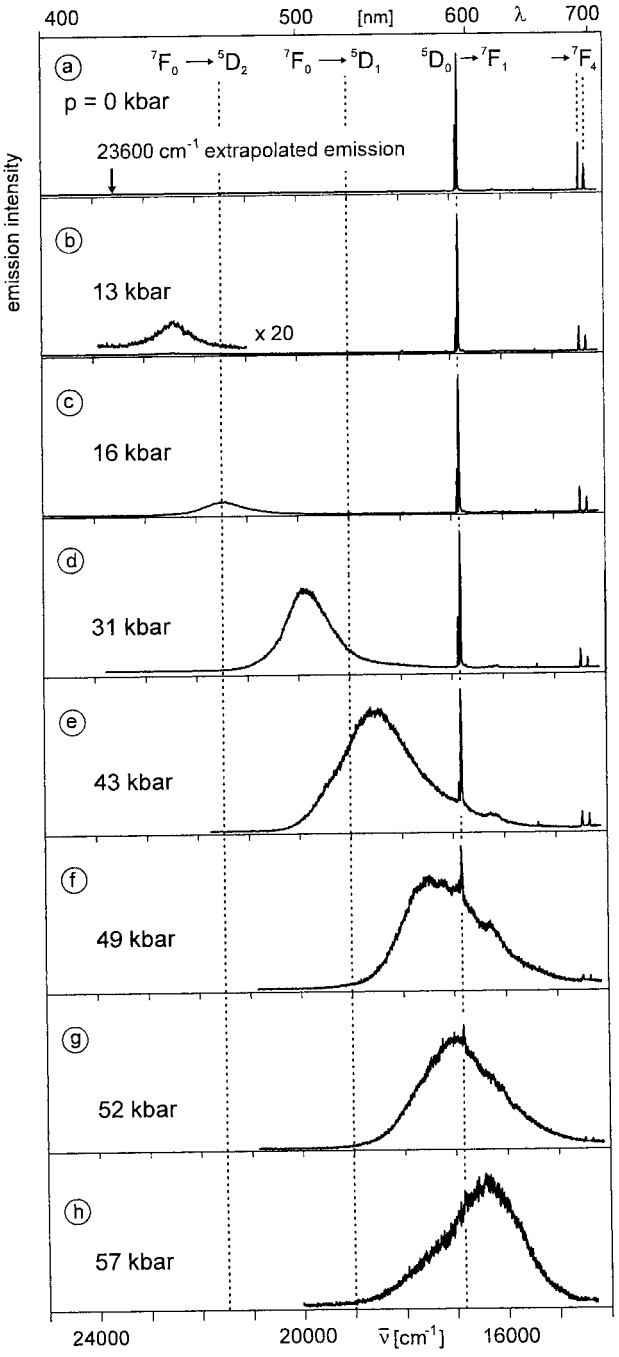

Figure 1. Emission spectra of single-crystal $Eu[Au(CN)_2]_3\cdot 3H_2O$ at various pressures ($T = 20$ K, $\lambda_{exc} = 363.8$ nm). With increasing pressure, the energy transfer from the dicynoaurates(I) (donors) to the Eu(III) acceptors can successively be tuned off. The vertical lines characterize positions of Eu^{3+} absorptions and emissions, respectively. More detailed Eu^{3+} emission spectra are shown in Figures 3 and 5.

This knowledge will help us to identify the most probable acceptor term of Eu^{3+} at ambient pressure for a resonant energy transfer (see section 3.4).

3.3. Eu^{3+} Acceptor Lines. At ambient pressure, the emission spectrum of $Eu[Au(CN)_2]_3\cdot 3H_2O$ consists only of a line structure, which dominates up to a relatively high pressure (Figure 1). These lines are immediately assigned to result from Eu^{3+}. (Compare also ref 13.) Generally, the electronic energies of the rare earth f−f transitions are only moderately influenced by the surrounding ligands, and since the crystal field splittings are relatively small (order of 10^2 cm^{-1}), one can use the literature assignments given for Eu^{3+} to classify also the lines

(35) Stock, M.; Yersin, H. *Solid State Commun.* **1978**, *27*, 1305.
(36) Yersin, H.; Hidvegi, I.; Gliemann, G.; Stock, M. *Phys. Rev.* **1979**, *B19*, 177.
(37) Bullett, D. W. *Solid State Commun.* **1978**, *27*, 467.
(38) Whangbo, M.-H.; Hoffmann, R. *J. Am. Chem. Soc.* **1978**, *100*, 6093.
(39) Messmer, R. P.; Salahub, D. R. *Phys. Rev. Lett.* **1975**, *35*, 533.
(40) Yersin, H.; Gliemann, G.; Rössler, U. *Solid State Commun.* **1977**, *21*, 915.
(41) Ziegler, T.; Nagle, J. K.; Snijders, J. G.; Baerends, E. J. *J. Am. Chem. Soc.* **1989**, *111*, 563.
(42) Dolg, M.; Pyykkö, P.; Runeberg, N. *Inorg. Chem.* **1996**, *35*, 7450.

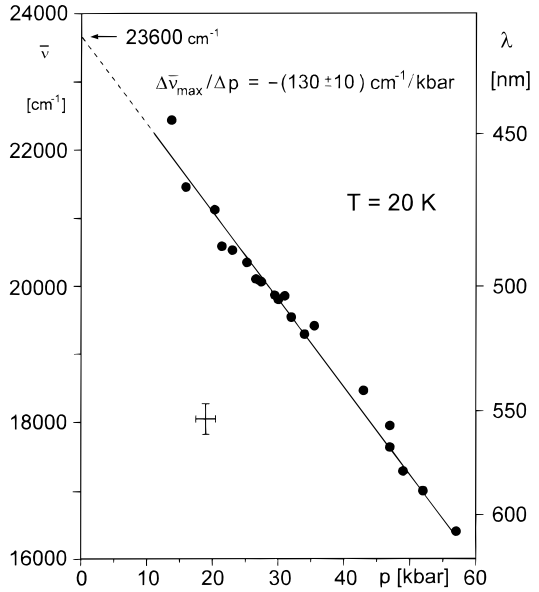

Figure 2. Pressure-induced shift of the dicyanoaurate(I) emission maxima of single-crystal $Eu[Au(CN)_2]_3 \cdot 3H_2O$ at $T = 20$ K. The emission at $p = 0$ kbar is quenched by a radiationless energy transfer. An extrapolation gives a value of 23 600 ± 300 cm^{-1} for $p = 0$ kbar.

observed here, even though the ion is sitting in a different environment. Figure 3 shows the main spectral region of the Eu^{3+} line emission on an enlarged wavenumber scale. The crystals were excited at the same wavelength (363.8 nm) used to measure the spectra of Figure 1, but the temperature was lowered to 1.2 K. The dominating lines are—on the basis of Eu^{3+} ion terms—assignable to $^5D_0$ emissions by comparing the transition energies of the groups of lines found here to the energies and classifications reported in the literature (for example, see refs 43−47). However, a detailed inspection of the spectrum (Figure 3) shows that a straightforward classification is not feasible if an emission from $^5D_1$ is not taken into account. Its position (or more exactly the position of the lowest crystal field sublevel) lies at 19 003 cm^{-1} (see Table 1).

As expected, one observes distinctly different time developments for the two emitting states $^5D_0$ and $^5D_1$. This is depicted in Figure 4. After a pulsed excitation at the energy of the transition $^7F_0 \rightarrow {}^5D_1$ the $^5D_1$ state emits with a monoexponential decay of 250 μs as is shown, for example, for the $^5D_1 \rightarrow {}^7F_3$ emission at 17 105 cm^{-1} (Figure 4, inset a). On the other hand, the emission detected at 16 851 cm^{-1} ($^5D_0 \rightarrow {}^7F_1$) exhibits a rise of 250 μs, corresponding to the population time of $^5D_0$ from $^5D_1$. This initial rise is followed by a monoexponential decay of 350 μs (Figure 4, inset b). The same characteristic time behavior is also found for all $^5D_1$ and $^5D_0$ emissions, respectively, and therefore, may be used to assign the various Eu^{3+} lines.

More elegant, however, are the measurements of time-resolved emission spectra, by which the $^5D_1$ emission can be well separated from the $^5D_0$ emission. Before these spectra, shown in Figure 5c,d, are discussed, it is suitable to address to an interesting phenomenon with regard to relaxation paths between the higher lying excited states.

Table 1. Eu^{3+} Lines for $Eu[Au(CN)_2]_3 \cdot 3H_2O$ at $T = 1.2$ K and $p = 0$ kbar

transn energy (cm^{-1})	assignt	transn energy for Eu^{3+} in $LaCl_3$[a,b] (cm^{-1})
21 484[c]	$^5D_2 \rightarrow {}^7F_0$	21 494
19 013[c]	$^5D_1 \rightarrow {}^7F_0$	19 034
19 003[d]		19 025
17 250[e]	$^5D_0 \rightarrow {}^7F_0$	17 267
18 671	$^5D_1 \rightarrow {}^7F_1$	18 670
		18 620
17 961	$^5D_1 \rightarrow {}^7F_2$	18 003
17 951		17 997
		17 941
17 105	$^5D_1 \rightarrow {}^7F_3$	17 178
17 056		17 163
		17 145
		17 125
		17 105
16 888	$^5D_0 \rightarrow {}^7F_1$	16 912
16 851		16 862
16 180	$^5D_0 \rightarrow {}^7F_2$	16 245
		16 239
		16 183
16 241	$^5D_1 \rightarrow {}^7F_4$	16 274
16 113		16 192
15 952		16 158
		16 122
		15 984
15 366	$^5D_0 \rightarrow {}^7F_3$	15 420
15 348		15 405
		15 387
		15 366
		15 347
15 159	$^5D_1 \rightarrow {}^7F_5$	15 223
14 977		15 186
14 929		15 181
		15 107
		15 068
		15 032
		15 015
14 482	$^5D_0 \rightarrow {}^7F_4$	14 516
14 372		14 434
14 357		14 400
		14 364
		14 226

[a] Data taken from ref 44 for comparison. [b] The regions of transitions found for the different compounds are correlated, but not the individual lines. [c] Lines only observed in excitation spectra. [d] Observed in emission and excitation spectra. [e] Estimated with an accuracy of ±20 cm^{-1} (see text).

Figure 5a reproduces part of the (usual) time-integrated Eu^{3+} emission spectrum. This spectrum corresponds to the one shown in Figure 3. For the excitation of these spectra, the wavelength of $\lambda_{exc} = 363.8$ nm ($\hat{=}$27 488 cm^{-1}) was chosen. At this energy the dicyanoaurate(I) layers absorb, and the energy is transferred nonradiatively to Eu^{3+} (see section 3.4). When, on the other hand, $^5D_1$ (at 19 003 cm^{-1} $\hat{=}$ 526.23 nm) is excited (Figure 5b), the $^5D_1$ emission becomes about 60 times more intense (relative to the $^5D_0 \rightarrow {}^7F_1$ emission). Obviously, after a UV excitation, $^5D_1$ is not effectively occupied, and the relaxation path preferentially populates $^5D_0$. The occurrence of specific relaxation paths is not unusual. Recently, such effects were investigated for Pt(II) and Ru(II) complexes.[48] Interestingly, this preference seems to become even more distinct under

(43) Yersin, H. *J. Chem. Phys.* **1978**, *68*, 4707.
(44) Dieke, G. H. *Spectra and energy levels of rare earth ions in crystals*; Wiley-Interscience Publishers: New York 1968.
(45) Flint, C. D.; Stewart-Darling, F. L. *Mol. Phys.* **1981**, *44*, 61.
(46) Huang, J.; Loriers, J.; Porcher, P. *J. Solid State Chem.* **1983**, *48*, 333.
(47) Richardson, F. S.; Reid, M. F.; Dallara, J. J.; Smith, R. D. *J. Chem. Phys.* **1985**, *83*, 3813.
(48) Schmidt, J.; Strasser, J.; Yersin, H. *Inorg. Chem.* **1997**, *36*, 3957.

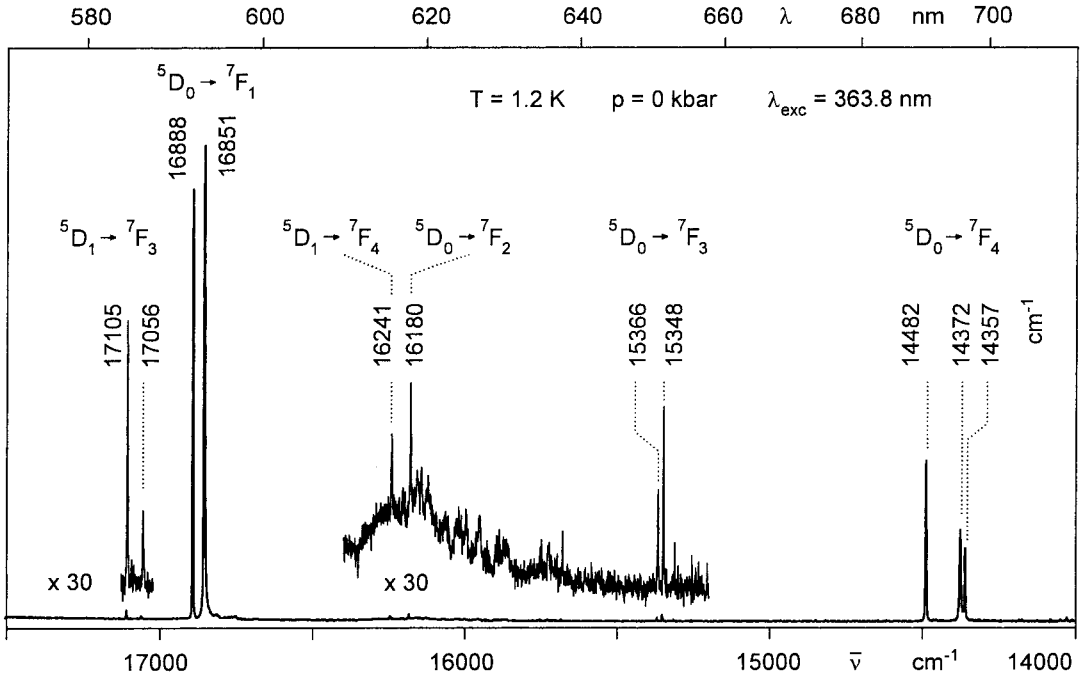

Figure 3. Eu^{3+} emission of $Eu[Au(CN)_2]_3 \cdot 3H_2O$ in the spectral range between 17 500 and 14 000 cm^{-1} at $T = 1.2$ K and $p = 0$ kbar. $\lambda_{exc} = 363.8$ nm ($\hat{=}27\,488$ cm^{-1}). The assignments are carried out by use of time-resolved spectra shown in Figure 5.

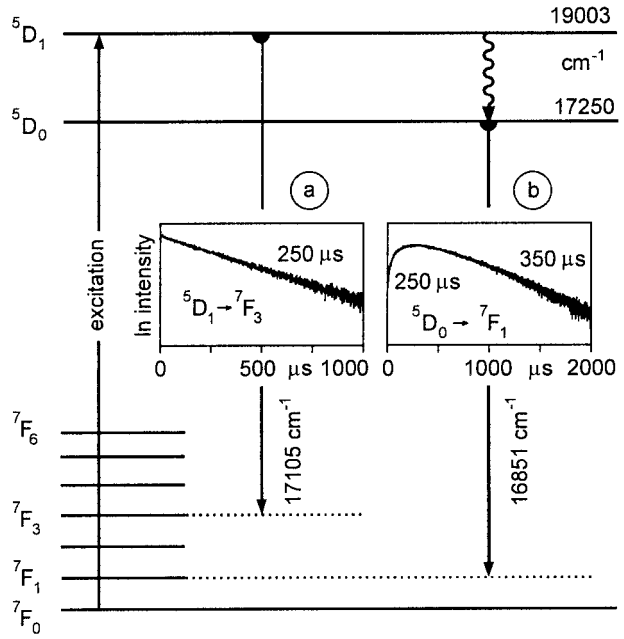

Figure 4. Schematic diagram to show the different emission rise and decay properties of the $^5D_1$ and $^5D_0$ states of Eu^{3+} in $Eu[Au(CN)_2]_3 \cdot 3H_2O$. $^7F_0 \rightarrow {}^5D_1$ (19 003 cm^{-1}) is excited by a pulsed (12 ns) and exactly tuned dye laser. (a) A detection at 17 105 cm^{-1} ($^5D_1 \rightarrow {}^7F_3$) results in a monoexponential decay of 250 μs, while (b) a detection at 16 851 cm^{-1} ($^5D_0 \rightarrow {}^7F_1$) leads to an emission rise of 250 μs and a decay of 350 μs, at $T = 1.2$ K and $p = 0$ kbar. The position of $^5D_0$ results from an estimate with an error of ± 20 cm^{-1} (see text).

application of high pressure (see below). Figure 5c reproduces the time-resolved emission spectrum, which is recorded in the short-time limit with no delay with respect to the laser pulse ($t = 0$ μs) and with a time window of $\Delta t = 7$ μs. Since the excitation energy is chosen to excite directly $^5D_1$ (at 19 003 cm^{-1}), the $^5D_0$ term is not yet strongly populated (compare Figure 4b), and the emission spectrum is dominated by $^5D_1$ lines. These lines are assigned by the use of literature data from refs 44−47. If, on the other hand, a delay of $t = 2$ ms is selected, $^5D_1$ is much more depopulated than $^5D_0$, due to a faster $^5D_1$ decay, and thus one mainly observes $^5D_0$ lines, as is demonstrated in Figure 5d. Due to the fact that the decay times of both terms are not very different, both emissions cannot be totally separated by time-resolved methods (but compare ref 48 for a different situation). However, the intensity changes between spectra c and d of Figure 5 are so drastic that the assignments to the different emitting terms are easily made. This procedure has been carried out for a larger spectral range than shown in Figure 5. The results and assignments are summarized in Table 1.

More detailed classifications of Eu^{3+} lines are available for well-defined site symmetries (e.g., see refs 45 and 47). However, in the context of the present investigation, it is not reasonable to try to achieve this detailed level of assignment since, in particular, the crystal structure and thus the site symmetry of Eu^{3+} are not known. Further, crystal field calculations are not available, and energies of vibrations and phonons of $Eu[Au(CN)_2]_3 \cdot 3H_2O$, which might appear as vibronic satellites, have not yet been determined. Nevertheless, some additional remarks seem to be appropriate. In this respect, we want to restrict ourselves to the spectral region below 17 500 cm^{-1} (Figure 3), in which mainly $^5D_0$ emissions are observed (due to the UV excitation).

$^5D_0 \leftrightarrow {}^7F_0$. For the compound investigated, this transition could not be found, since it is too weak. However, its position may be estimated from a comparison of $^5D_1 \rightarrow {}^7F_J$ with $^5D_0 \rightarrow {}^7F_J$ transitions to 17 250 $\pm$ 20 cm^{-1}. The weakness of the transition $^5D_0 \leftrightarrow {}^7F_0$ indicates that the Eu^{3+} ion occupies a site of high symmetry, which is only weakly distorted.

The Eu^{3+} emission lines observed at 17 056 and 17 105 cm^{-1} might easily be taken as $^5D_0 \rightarrow {}^7F_0$ origins of two additional sites. However, the time behavior measured for these lines excludes such an assignment (compare spectra c and d in Figure 5), and the classification as $^5D_1 \rightarrow {}^7F_3$ follows immediately from a comparison with literature[44−47] data. Interestingly, both lines disappear with an application of a pressure of $p > 20$ kbar. Presumably, this indicates that the rate of relaxation from $^5D_1$

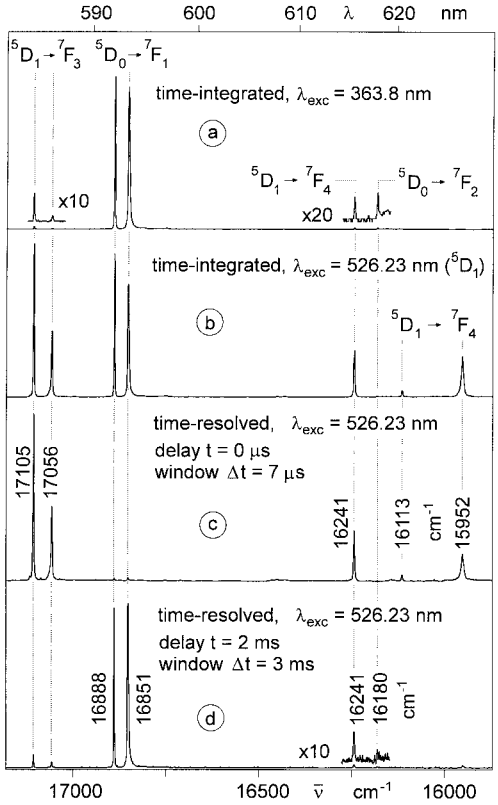

Figure 5. Time-integrated and time-resolved emission spectra of Eu^{3+} in $Eu[Au(CN)_2]_3 \cdot 3H_2O$ at $T = 1.2$ K and $p = 0$ kbar. Only a reduced part of the spectrum compared to the one shown in Figure 3 is reproduced: (a) time-integrated (= usual) emission excited at $\lambda_{exc} =$ 363.8 nm (excitation of the donor layers) (compare Figure 3); (b) time-integrated emission excited at $\lambda_{exc} = 526.23$ nm ($^7F_0 \rightarrow {}^5D_1$); (c) time-resolved *fast* emission measured during the first 7 μs (delay time $t =$ 0 μs, time window $\Delta t = 7$ μs) (compare the emission time development shown in Figure 4), excitation at $\lambda_{exc} = 526.23$ nm ($^7F_0 \rightarrow {}^5D_1$) with a 12 ns pulse; (d) time-resolved emission measured after a delay time of $t = 2$ ms with a time window of $\Delta t = 3$ ms. Excitation as in (c).

to $^5D_0$ increases with pressure. Indications for a similar behavior have already been reported.[49]

$^5D_0 \rightarrow {}^7F_1$. The two lines at 16 851 and 16 888 cm^{-1} ($p =$ 0 kbar) are the most intense Eu^{3+} lines observed after UV excitation. They are assigned to $^5D_0 \rightarrow {}^7F_1$ transitions. These are often discussed in connection with a magnetic dipole allowedness[46,50] and therefore are—according to ref 46—usually not associated with significantly intense vibronic satellites. With a pressure increase from zero to about 10 kbar, the 16 851 cm^{-1} line splits by about 16 cm^{-1} (Table 2). Since $^7F_1$ is 3-fold degenerate, this splitting leads to the three components expected to occur in a low-symmetry situation. This behavior indicates again a high site symmetry for Eu^{3+} at ambient pressure, which allows the occurrence of at least doubly degenerate states.

$^5D_0 \rightarrow {}^7F_2$. In the region between 15 500 and 16 300 cm^{-1}, one observes at $p = 0$ kbar one weak line at 16 180 cm^{-1} and a number of weak and broad transitions, which are assigned to the $^5D_0 \rightarrow {}^7F_2$ manifold (Figure 3). These transitions exhibit a so-called hypersensitivity with respect to changes in the environment (e.g., see refs 51 and 52). Often, important vibrational satellites are found in this region due to distinct vibronic coupling.[45,46] Possibly, several of these weak transitions may be assigned to vibronic lines. Interestingly, with increasing pressure from zero to about 40 kbar, the intensity in this region increases by a factor of about 50 (normalized to the low-energy $^5D_0 \rightarrow {}^7F_1$ component). Apparently, this effect displays the hypersensitivity of the $^5D_0 \rightarrow {}^7F_2$ transitions(s) (Figure 1). For completeness, it is referred to the time-resolved spectra (Figure 5c,d), which show that the line at 16 241 cm^{-1} does not result from $^5D_0$ but has to be assigned to $^5D_1 \rightarrow {}^7F_4$.

Table 2. Pressure-induced Shifts of Eu^{3+} Emission Lines

	$Eu[Au(CN)_2]_3 \cdot 3H_2O$[a]		$Na_5\,Eu(MoO_4)_4$ [c),d]	
region	lines[b] (cm^{-1})	$\Delta\bar{\nu}/\Delta p$[b] (cm^{-1}/kbar)	lines (cm^{-1})	$\Delta\bar{\nu}/\Delta p$ (cm^{-1}/kbar)
$^5D_1 \rightarrow {}^7F_3$	17 105[e]	−0.94		
	17 056[e]			
$^5D_0 \rightarrow {}^7F_1$	16 888	−0.84	16 870	−−0.96
	16 851[f]	−0.78	16 815	−−0.72
$^5D_0 \rightarrow {}^7F_2$	16 180		16 464	−1.10
			16 302	−0.50
			16 201	−0.44
$^5D_0 \rightarrow {}^7F_3$	15 366		15 272	−0.76
	15 348	−0.70	15 264	−0.86
$^5D_0 \rightarrow {}^7F_4$	14 482[g]	−0.31[g]	14 280	−0.98
	14 372	−0.74	14 215	−1.08
	14 357	−0.76		

[a] $T = 20$ K; this work. [b] At $p = 0$ kbar. Errors: ±1 cm^{-1}; ±0.1 cm^{-1}/kbar. [c] $T = 298$ K; from ref 53. [d] The regions of emissions found for the two compounds are correlated, but not the individual lines. [e] Lines disappear for $p > 20$ kbar. [f] Line splits by ≈16 cm^{-1} up to $p = 10$ kbar. [g] Line splits by ≈10 cm^{-1} up to $p = 10$ kbar. The red shift is given for the baricenter.

$^5D_0 \rightarrow {}^7F_3$, $^7F_4$. At $p = 0$ kbar, two lines at 15 348 and 15 366 cm^{-1} are observed in the region of the $^5D_0 \rightarrow {}^7F_3$ transitions (Figure 3). The high-energy line disappears with increasing pressure. In the region of the $^5D_0 \rightarrow {}^7F_4$ transitions, one can measure at least three relatively strong lines at 14 357, 14 372, and 14 482 cm^{-1} ($p = 0$ kbar, Figure 3). Upon application of a relatively small pressure (≈5 kbar), one observes a splitting of the 14 482 cm^{-1} line and a distinct intensity reduction of the 14 372 cm^{-1} line (relative to the intensity of the 14 357 cm^{-1} line). Possibly, this behavior indicates again that at ambient pressure the effective symmetry at the Eu^{3+} site is still sufficiently high not to lift all degeneracies.

All Eu^{3+} lines observed exhibit a red shift with application of high pressure (Table 2). The $\Delta\bar{\nu}(Eu^{3+})/\Delta p$ values lie between −0.7 and ≈−1.0 cm^{-1}/kbar. They compare well with values, for example, determined for $Na_5Eu(MoO_4)_4$[53] (compare also refs 54−56). In a number of investigations, detailed explanations for the occurrence of pressure-induced shifts have been given on the basis of changes of the free-ion Slater parameters, spin−orbit coupling constants, and crystal field parameters including nephelauxetic effects.[53−57] These approaches seem to be quite successful, but as already pointed out, a similarly detailed approach is not yet possible for $Eu[Au(CN)_2]_3 \cdot 3H_2O$. Moreover, one problem has, to our knowledge, not yet been taken into account. For a vibronic line, the pressure-induced shift consists additionally of a blue shift of the vibrational energy,

(49) Hayes, A. V.; Drickamer, H. G. *J. Chem. Phys.* **1982**, *76*, 114.
(50) Serra, O. A.; Thompson, L. C. *Inorg. Chem.* **1976**, *15*, 504.
(51) Mason, S. F.; Peacock, R. D.; Stewart, B. *Mol. Phys.* **1975**, *30*, 1829.
(52) Stręk, W. *Theor. Chim. Acta* **1979**, *52*, 45.
(53) Changxin, G.; Bilin, L.; Yuefen, H.; Hongbin, C. *J. Lumin.* **1991**, *48/49*, 489.
(54) Huber, G.; Syassen, K.; Holzapfel, W. B. *Phys. Rev.* **1977**, *B15*, 5123.
(55) Qiuping, W.; Lijun, L.; Dingzheng, Z.; Yuanbin, C.; Lizhong, W. *J. Phys.: Condens. Matter* **1992**, *4*, 6491.
(56) Chen, G.; Haire, R. G.; Peterson J. R.; Abrahm, M. M. *J. Phys. Chem. Solids* **1994**, *55*, 313.

which often lies in the range $1-2$ cm^{-1}/kbar,[58] and thus, besides the opposite sign, is even slightly larger than the values determined for purely electronic shifts. Therefore, if vibronic coupling is not taken into account, a detailed and quantitative description of pressure-induced energy shifts can easily fail.

3.4. Tunable Energy Transfer. At ambient pressure, the $[Au(CN)_2]_n^{n-}$ donor emission is totally quenched due to an effective radiationless energy transfer to the Eu^{3+} acceptors (Figure 1a), while without energy transfer the dicyanoaurate(I) emission is always very intense.[8,9] This indicates the significance of a resonant transfer process. The transfer rate P_{D-A} between donor D and acceptor A can be expressed by[59-62]

$$P_{D-A} = F(R) \int f_D^e(\bar{\nu})\, f_A^a(\bar{\nu})\, d\bar{\nu}$$

The integral is the important spectral overlap integral of the donor emission $f_D^e(\bar{\nu})$ with the acceptor absorption profile $f_A^a(\bar{\nu})$, and it describes the resonance condition. Both functions are normalized according to $\int f_D^e(\bar{\nu})\, d\bar{\nu} = \int f_A^a(\bar{\nu})\, d\bar{\nu} = 1$. $F(R)$ summarizes the essential mechanism(s), like the Dexter[60] exchange or the Förster[59,62] multipole mechanism with their specific distance (R) dependencies.

From the extrapolation shown in Figure 2 for $T = 20$ K, one expects that at ambient pressure the maximum of the dicyanoaurate(I) emission lies at $23\,600 \pm 300$ cm^{-1} without energy transfer. From the information given in refs 8, 9, 14, and 31 it is estimated that the emission bandwidth (e.g. taken at one-tenth of the maximum intensity) is of the order of 2000 cm^{-1}. From these data it follows that the resonance transfer (nonzero spectral overlap integral) may involve the $^5L_6$ state of Eu^{3+}, having its baricenter near 25 100 cm^{-1}, for example, in $Cs_2Na[EuCl_6]$.[47] However, a very good spectral overlap will occur with the $^7F_0 \rightarrow {}^5D_3$ absorptions, which have their baricenter in the same Eu^{3+} chloride complex near 24 300 cm^{-1}.[47] (Compare also ref 13.) Moreover, the results show (Figures 1a and 3) that mainly $^5D_0$ emits. This means that after an energy transfer the rates of relaxation at the Eu^{3+} center to the emitting $^5D_0$ state are distinctly larger than the radiative decay rates of higher lying states. (Compare also ref 48.) This relaxation, in particular from $^5D_1$ to $^5D_0$, becomes even more effective under high-pressure application.

With a pressure increase up to $p \approx 10$ kbar, one can shift the low-lying states of the dicyanoaurates(I) relative to the acceptor states by more than 10^3 cm^{-1}, and an emission from the dicyanoaurates(I) appears (Figures 1b and 2). The very small shift of the Eu^{3+} lines of less than -1 cm^{-1}/kbar (Table 2) may be disregarded in this respect. Obviously, the spectral overlap with the $^5L_6$ and $^5D_3$ absorptions is tuned off or is at least strongly reduced. In this context, it is important to note that the emission intensity is still relatively weak (Figure 1b) and that its bandwidth is smaller than expected from a comparison to $M[Au(CN)_2]$ compounds with no energy transfer.[1-9,14] An explanation will be given below.

A pressure increase to $p = 16$ kbar leads to a further red shift of the donor emission and to an intensity increase by more than a factor of 10 (normalized to the intensity of the $^5D_0 \rightarrow {}^7F_1$ emission), although the spectral overlap reaches a maximum with the $^7F_0 \rightarrow {}^5D_2$ absorptions (Figure 1c). Obviously, the higher lying Eu^{3+} states represent more effective acceptors than $^5D_2$.

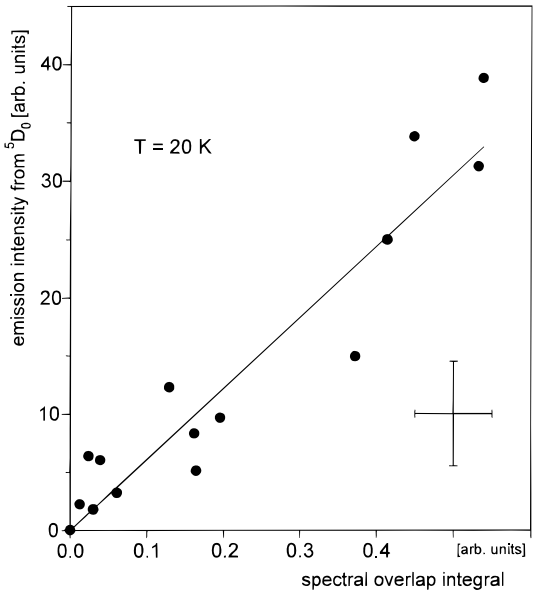

Figure 6. Integrated $^5D_0$ emission intensity (all lines) versus the spectral overlap integral of the dicyanoaurate(I) (donor) emission with the $^7F_0 \rightarrow {}^5D_1$ Eu^{3+} acceptor absorption of $Eu[Au(CN)_2]_3 \cdot 3H_2O$ (for details see section 3.4). The results are only valid for $30 \le p \le 60$ kbar. $\lambda_{exc} = 363.8$ nm.

The situation becomes more defined with respect to the spectral overlap, when the pressure exceeds $p \approx 30$ kbar. Then, the spectral overlap of the donor emission with absorptions to $^5D_2$ and higher lying states is tuned off. Thus, a further pressure increase shifts the donor emission continuously into the range of the $^7F_0 \rightarrow {}^5D_1$ acceptor absorption (Figure 1d). In this situation, it is expected that the efficiency of an energy transfer depends linearly on the value of the spectral overlap integral. Indeed, Figure 6 shows the anticipated dependence for the intensity of the integrated $^5D_0$ emission. This demonstrates that the radiationless energy transfer to the $^5D_1$ state can continuously be tuned on and subsequently tuned off. A similar behavior with respect to such a tunability has so far only been found for the related $Eu_2[Pt(CN)_4]_3 \cdot 18H_2O$ and $Sm_2[Pt(CN)_4]_3 \cdot 18H_2O$ compounds.[16,17]

Interestingly, when the spectral overlap with the $^5D_1$ absorption is tuned to zero, the energy transfer is—within limits of the experimental accuracy—tuned off, although an overlap with the $^5D_0$ absorption reaches a maximum. Obviously, $^5D_0$ does not act as acceptor term. This behavior is in contrast to the situation observed for $Eu_2[Pt(CN)_4]_3 \cdot 18H_2O$, for which $^5D_0$ represents an effective acceptor term. A selectivity with respect to the acceptor states does not seem to be unusual. It has also been observed for $Sm_2[Pt(CN)_4]_3 \cdot 18H_2O$, where higher lying states are good acceptors, but the $^6H_{5/2} \rightarrow {}^4G_{5/2}$ absorption does not act as acceptor even with a high spectral overlap.[17] Possible explanations for these selectivities are briefly discussed in ref 17, but these effects require further studies.

Besides the properties of the states involved, the effective mechanism of energy transfer is largely determined by the structure of the system. In $Eu[Au(CN)_2]_3 \cdot 3H_2O$, the nitrogen atoms of the CN^- ligands of the $[Au(CN)_2]^-$ complexes coordinate directly to the Eu^{3+} cations. (Compare ref 13.) Further, since the low-lying states of the dicyanoaurates(I) may

(57) Gregorian, T.; d'Amour-Sturm, H.; Holzapfel, W. B. *Phys. Rev.* **1989**, *B17*, 12497.
(58) Yersin, H.; Braun, D.; Trümbach, D. In *Book of Abstracts*, Tenth International Conference on Photochemical Conversion and Storage of Solar Energy; Calzaferri, G., Ed.; 1994; p 319.
(59) Förster, T. *Fluoreszenz Organischer Verbindungen*; Vandenhoeck und Ruprecht: Göttingen, Germany, 1951.
(60) Dexter, D. L. *J. Chem. Phys.* **1953**, *21*, 836.
(61) Reisfeld, R. *Struct. Bonding* (*Berlin*) **1976**, *30*, 65.
(62) Watts, R. K. In *Optical properties of ions in solids*; DiBartolo, B., Ed.; Plenum Press: New York, 1975; p 307.

be traced to the Au 6p, CN π^* LUMO and since this MO is spread out significantly even beyond the nitrogen atoms (compare MO contour plots shown in refs 22, 27, and 63), it is seen that the wave functions of the donor states considerably overlap also with the 4f orbitals of the Eu^{3+} acceptors. Therefore, it is expected that the Dexter exchange mechanism strongly dominates and that the transfer rates are very large.[60] A similar conclusion has been drawn for the related tetracyanoplatinates(II),[16−18,43] where, indeed, transfer rates of the order of 10^9 s^{-1} are found.[64]

If a transfer rate of a similar order of magnitude is also effective in $Eu[Au(CN)_2]_3 \cdot 3H_2O$, where the donor state or states exhibit an emission decay rate of the order of 10^4 s^{-1} (without energy transfer; compare ref 31), the donor emission should be totally quenched, as long as energy transfer is possible. However, the results presented in the Figure 1b−h show that this is not the case. On the other hand, it has to be taken into account that a total quenching will only occur if the donor emission results from sufficiently coupled states. However, according to the discussions in section 3.1 and in ref 9, this condition is not fulfilled. The very broad emission bands of the dicyanoaurates(I) are better described as consisting of overlapping and (nearly) independent emissions of different $[Au(CN)_2]_n^{n-}$ clusters, where the cluster size n is still unknown. Thus, the donor emission is strongly inhomogeneously broadened. Under suitable conditions of a nonvanishing spectral overlap between the donor emissions of specific clusters with an Eu^{3+} acceptor absorption, energy transfer occurs, and the emissions of these specific clusters are quenched, while—in the case of a short-range process, like the Dexter exchange mechanism—other clusters are not influenced. In this model, one would expect that a spectral shift of the inhomogeneously broadened donor emissions over different acceptor terms would have a distinct influence on the emission bandwidths. Indeed, this is indicated by the spectra shown in Figure 1b−h. Gradually tuning off the energy transfer the half-width of the dicyanoaurate(I) emission increases from ≈800 to ≈2400 cm^{-1}. For completeness, it is mentioned that, with increasing pressure, the inhomogeneity within the high-pressure chamber will also increase (e.g., see refs 9 and 14). This effect is also displayed in the half-widths of the ruby lines used for the pressure determination, but these exhibit a considerably smaller increase relative to the values at zero pressure than found for the dicyanoaurate(I) emission. Thus, the model presented seems to describe the properties of $Eu[Au(CN)_2]_3 \cdot 3H_2O$ appropriately.

4. Conclusion

The extremely high energy tunability of the low-lying electronic states of the dicyanoaurate(I) layers under high pressure is a consequence of the specific structure type of this class of compounds. Due to the two-dimensional arrangements of the $[Au(CN)_2]^-$ complexes, electronic energy bands are formed. A relatively small decrease of the Au−Au separations leads to a significant reduction of the band gap energy and thus also to a large red shift of the lowest electronic transitions. In $Eu[Au(CN)_2]_3 \cdot 3H_2O$, the emission from these states is efficiently quenched by a radiationless energy transfer presumably according to a resonant Dexter process to the Eu^{3+} acceptor state(s) $^5D_3$ (and presumably $^5L_6$) at ambient pressure. With a pressure increase, the donor emission can be tuned in and may be shifted over several thousand wavenumbers. This allows one to continuously tune the resonance condition (spectral overlap integral) for the radiationless energy transfer. Thus, after $^5D_3$, successively $^5D_2$ and $^5D_1$ become acceptor terms though with smaller efficiencies. Interestingly, $^5D_0$ does not act as an acceptor term. Moreover, indications are found that a high pressure increase also has an influence on the relaxation paths and/or rates, determining the relative populations of $^5D_1$ and $^5D_0$. Furthermore, in the medium-pressure range, the acceptor quenches part of the inhomogeneous emission band with a distinct reduction of the emission bandwidth. This behavior supports an earlier report[9] on the occurrence of $[Au(CN)_2]_n^{n-}$ clusters. However, the latter properties require further studies.

Note Added in Proof. A recent determination of the crystal structure of $Eu[Au(CN)_2]_3 \cdot nH_2O$ at room temperature yielded for the Eu^{3+} center a D_{3h} point group symmetry (space group $P\bar{6}2m$, No. 189).[65] In this symmetry degenerate states may occur. Thus this result fits nicely to the symmetry predictions given for the electronic states of Eu^{3+}.

Acknowledgment. Financial support of the Fonds der Chemischen Industrie, the Deutsche Forschungsgemeinschaft, and NATO is gratefully acknowledged. Acknowledgment is also made to the donors of the Petroleum Research Fund, administered by the American Chemical Society, for support of this research.

IC980252P

(63) Sano, M.; Adachi, H.; Yamatera, H. *Bull. Chem. Soc. Jpn.* **1982**, *55*, 1022.

(64) von Ammon, W.; Yersin, H.; Gliemann, G. *Nuovo Cimento* **1981**, *63B*, 3.

(65) Stiel, A. M. Ph.D. Thesis, Universität Regensburg, 1996.